Domains and Effective Anisotropy in Ferromagnetic Metallic-Semiconductor Nanostructure

A. Zolanvari, H. Sadeghi*, J. Nezamdost
Physics Department, Arak University, Arak, Iran.

Abstract

Introduction: Structural and magnetic properties of ferromagnetic Fe thin layer films on Si substrates have been reported. We present topography features of these nanostructures films by atomic force microscopy (AFM). Characterization of magnetic domains and walls between them can be performed by using magnetic force microscopy (MFM) and alternating gradient field magnetometer (AGFM) instruments. The Fe thickness ranges from 50 to 150 nm. Our focus is to study systematically the effects of film thickness on magnetic anisotropy in thin films grown on semiconductor substrates. MFM images reveal stripe domain structure for the 100nm thick Fe on Si as well as hysteresis curves. The effective anisotropy shows oscillation for two types of Si substrates when the Fe films thickness increased.

Aim: Our focus is to investigate systematically the effect of film thickness on magnetic hysteresis and effective anisotropy, especially in thin films grown on semiconductors substrates. For revealing stripe domain structure of Fe/Si (100) and Fe/Si (111), we use MFM pictures as well as hysteresis curves.

Material and method: Fe thin films were deposited by thermal evaporation. Iron ingots from a 99.99 % purified Fe powder evaporated using an electron gun. The deposited Fe layer thicknesses vary from 50 to 150 nm. The crystalline structure of the deposited structures, X-ray diffraction method was used for investigation of nanostructure. Magnetic properties were also measured with MFM and experimental hysteresis loops were obtained by AGFM unit.

Results: For Fe layer with 50nm thickness, Fe on Si(100) and Si(111) substrates, the Fe grows with (110) texture and has a bcc structure. The coercive field measured for the Fe films is about 100Oe. The measured hysteresis loops show that the coercive field decreases while the saturation field increases and such uniaxial anisotropy increases with increasing step density.

Conclusion: Hysteresis diagrams show good ferromagnetic characteristics of these samples. The effective anisotropy shows oscillation, for two substrates Si types, when the Fe films thickness increased.

***Keywords*:** Magnetic nanostructure, Fe thin films, Magnetic properties, Magnetic anisotropy

Introduction

The knowledge and understanding of the magnetic nanostructures are large interest from fundamental as well as applied research. From the fundamental point of view, magnetic

*Corresponding author

domain observations can be used to verify domain models or nano-magnetic theories, to provide information about the intrinsic parameters of materials and their macroscopic properties.

The effect of substrates and under layers on the physical properties of Fe thin films has been thoroughly investigated. [1-8] Among the interesting properties of Fe thin films, magnetic anisotropy has attracted a lot of attention, mainly the existence of a positive (perpendicular) anisotropy. This anisotropy is explained either by a reduced Fe magnetization due to inter-diffusion which lowers the shape anisotropy or to a contribution of stress. As the thickness of a film is reduced, its properties are expected to be strongly influenced by surface and interfaces, which are inevitably rough at atomic scales. Roughness of surface and interface strongly also influence both the static magnetization and hysteresis magnetic properties of thin films.[9,10] The properties of isolated magnetic grains change considerably as their sizes enter the nanometer range. Particles smaller than the width of a domain wall (about 40 nm for bulk Fe) are in a single domain with the magnetization along the anisotropy axis. Experiments have demonstrated that surface steps induce an in-plane uniaxial magnetic anisotropy, with the easy axis parallel to the step direction, in a variety of magnetic thin films grown on metal as well as on semiconductor stepped surfaces.[11] In this paper, magnetic properties of ferromagnetic Fe thin film on two types of Si substrates have been reported. The main purpose is to study of structural and magnetic properties of ferromagnetic metallic thin film on semiconductor substrate. Magnetic domains and walls between them can be performed by MFM and AGFM devices.

Material and Method

Experimental Details

Fe thin films were grown on 1cm×1cm substrates by thermal evaporation. Before loading the samples into evaporation chamber, their surfaces were refreshed in diluted HF and cleaned by the standard procedures used in microelectronics technology. After evacuation down to 10^{-8} torr and prior to evaporation, Si wafers were annealed in situ, for 5 minuets at 800^{o}C. Iron ingots from a 99.99 % purified Fe powder evaporated using an electron gun, with 0.3-0.4 nm/s rate and at 10^{-8} torr pressure. The film thicknesses were also measured by vibrating quartz system. The Fe thicknesses vary from 50 to 150 nm.

To identify the crystalline structure of the deposited structures, X-ray diffraction (Cu-Kα radiation, λ= 0.15405 nm, Breg-Brentano geometry) method was used for investigation of structure. Magnetic properties were also measured with MFM and experimental hysteresis loops were obtained by AGFM unit.

Results and Discution

Fig. 1a and 1b show XRD patterns of Fe/Si(100) and Fe/Si(111), respectively. After deposition, for the Fe thin films on the two substrates(up to 50nm), no peaks were seen in the XRD spectra, which is due to distributed of randomly oriented grains, thus the peaks are too weak to be detected due to the sensitivity of the instrument and no diffraction peaks could be clearly seen in the spectra with corresponding to the results in Ref.[3]. For Fe layer with 50nm thickness, Fe on Si(100) and Si(111) substrates, the Fe grows with (110) texture and has a bcc structure, see Fig.1a and Fig.1b.

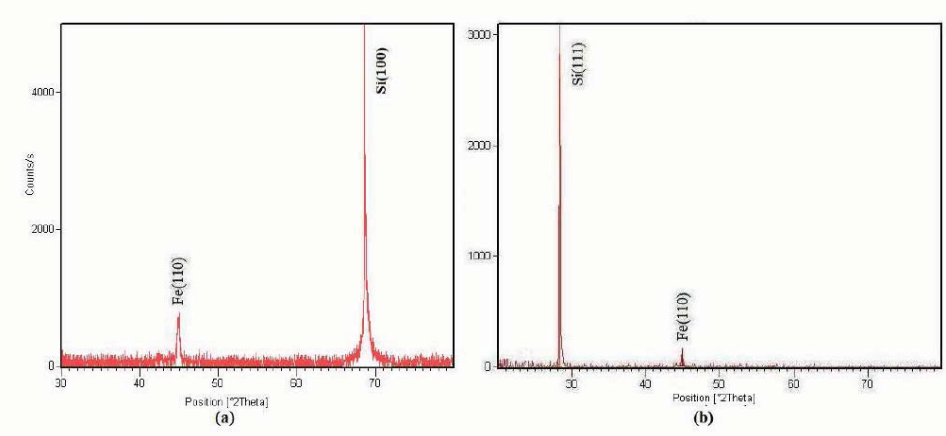

Figure. 1- XRD patterns of as deposited a) Fe/Si (100) and b) Fe/Si (111) thin nanostructures films.

The in-plane hysteresis loops of Fe films were measured by AGFM. The results are shown for different thicknesses of Fe on Si (100) and Si (111) substrates, in Fig. 2a and 2b, respectively. The coercive field measured for the Fe films is about 100Oe. The measured hysteresis loops show that the coercive field decreases while the saturation field increases when the external field is turned away from the direction parallel to the steps to the direction perpendicular to the steps, and such uniaxial anisotropy increases with increasing step density.[12] As the film thickness decreases, the fraction of soft phase increases substantially. Our results shown, the samples exhibit square hysteresis loops except for the film 50nm thickness.

The MFM pictures show distributed magnetic domains, as depicted in Fig. 3a and 3c for Fe thin films on Si (100) and Si (111) substrates with 100 nm thickness, respectively. MFM was operated in a non-contact, dual-pass lift-mode technique with commercially available, CoCr-coated Si MFM tips. The tips were perpendicularly magnetized and scan height was 25nm. In this image, one can see bright and dark areas that can be regarded as corresponding to the position of inner down and up domains.

The periodicity or the width of the domains depends on the field irradiation dose, ranging about 2-4 μm. For better illustration, in Fig. 3b and 3d, we show a zoom picture of the magnetic domain structures. Because of the small coercive field of the magnetic surface and the influence of the magnetic tip, we have observed that the magnetic domains distribution depends on the distance between tip and surface. We note that measurements on different magnetic samples indicate that the distance between the tip apex and the effective position of the magnetic moment in the tip depends on the magnetic properties of the measured surface and therefore the calculated magnetic moment from MFM data should be taken as a rough estimated only.[13]

The new systems must operate in high-temperature and high-frequency regimes that are inaccessible to conventional crystalline and amorphous magnetic materials. The need for increased energy efficiency requires reduced power loss from inductive components. Nanocrystalline magnetic materials hold promise for meeting these requirements without resorting to the trade-offs needed when using conventional materials.

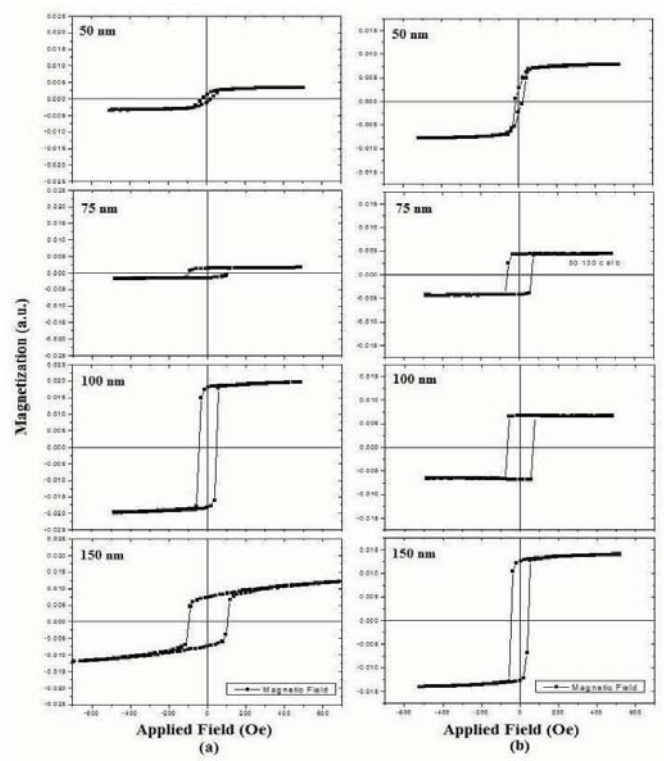

Figure. 2- Hysteresis loops of as deposited a) Fe/Si(100) and b) Fe/Si(111) Fe thin films films in different thicknesses.

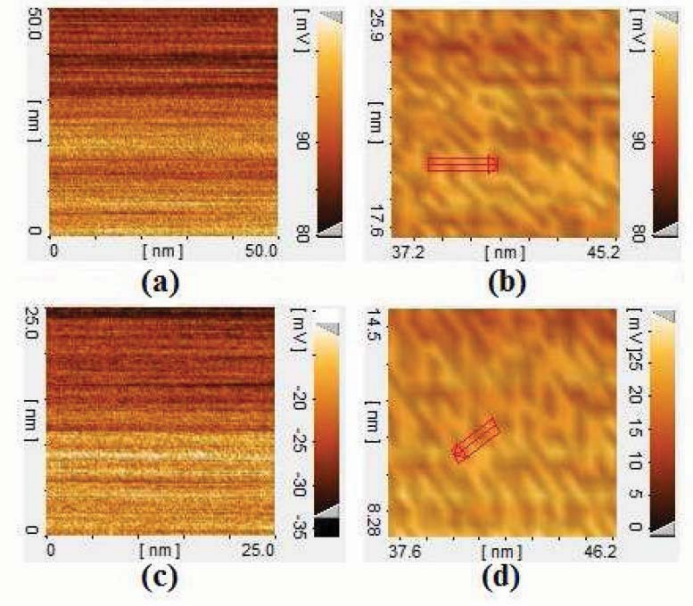

Figure 3- a) 50*nm*×50*nm* MFM scan of Fe layer with 100 nm thickness, on Fe/Si (100) b) Zoom in part of it, and c) 25*nm*×25*nm* MFM scan of Fe layer with 100 m thickness, on Fe/Si(111) d) Zoom in part of it.

A material that maintains a remnant magnetization, M_r, in the absence of an applied field is known as a ferromagnetic material. Ferromagnets are the most widely used type of magnet, and are typically referred to as magnetic materials or magnets. A finite field known as the coercive field, H_c, is used to reverse the M_r. When driven with an applied field a ferromagnet reaches a saturation magnetization, M_S, that is an intrinsic property of the material. The magnet's permeability, μ, reflects the ease with which it is magnetized and is an extrinsic property that depends on the microstructure of the material.

A magnet can be characterized by a plot known as a hysteresis loop (Fig. 4). H_c is measured as the width of the loop, M_s as the height of the loop, and μ as the slope in the first quadrant. The area of the loop corresponds to the energy stored in the material during the magnetization process.

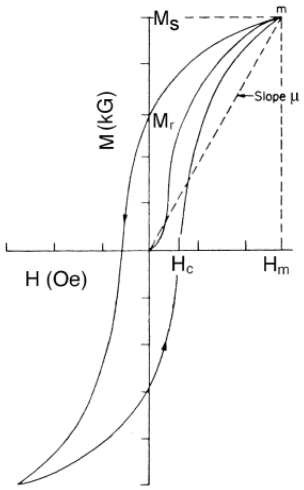

Figure 4- Example hysteresis loop illustrating coercivity (H_c), saturation magnetization (M_s), remnant magnetization (M_r), and permeability (μ).

The coercive field is influenced by a property known as magnetic anisotropy. This represents the force required to rotate the magnetization vector of a magnet out of its equilibrium direction. High anisotropy generally results in a high H_c, as the magnet experiences a resistance to switching it's magnetization direction. The magnetocrystalline anisotropy is generated from the crystalline symmetry of the magnet. Shape anisotropy results from the need to maintain a closed flux path around and through a magnet. Stress anisotropy results from residual or applied stress applied to the magnet.

In this case the film thickness is an important parameter, which has to be considered in the coupling volume over which the anisotropy is averaging, since the averaging will depend on the length scale perpendicular to the film plane. Therefore, we have taken the coupling volume over which the anisotropy should be averaged to be $V = Le^2 d$, where d is the film thickness and Le is the ferromagnetic exchange length determined as $Le = (A/K_1)^{1/2}$, where A is the exchange constant and K_1 is the first anisotropy constant.

Hence, the number of grains (crystallites) contained in the coupling volume is: [5,6]

$$N = \frac{L_e^{\,2} d}{D^3} \qquad (1)$$

where D is the average grain size. As the effective anisotropy *Keff* is given by[5,6]: *Keff* =*K*1*/N*. From this relation and Eq. (1) it follows that in the case of thin polycrystalline films the effective anisotropy is given by:

$$K_{eff} = \frac{K_1^2 D^3}{Ad}. \qquad (2)$$

The last expression is valid for the polycrystalline film grain size D is smaller than the exchange length *Le*. The relation between coercivity and effective anisotropy is given by:

$$H_c = \frac{p_c K_{eff}}{M_s} \qquad (3)$$

where *pc*= 0.64 is dimensionless pre-factor[6]. Thickness dependence of remnant magnetization, saturation magnetization, saturation field, coercivity, permeability and the effective anisotropy in Fe/Si(111) and Fe/Si(100) are given in table(1) and table(2), respectively. The *Keff* obtained values are plotted in Fig. 5 as a function of Fe thickness. It is also show its oscillation when thickness is increased for both Si(111) and Si(100) substrates.

Table. 1- Thickness dependence of remnant magnetization (M_r), saturation magnetization (M_s), saturation field (H_m), coercivity (H_c), permeability (μ) and the effective anisotropy in Fe/Si(111)

Thichness(nm)	M_r	M_s H_c	H_m	$\mu=M_s/H_m$	K_{eff}
50	0.0012	0.0027 20	94	0.0000287	0.596
75	0.00137	0.0015 100	200	0.0000075	1.243
100	0.0180	0.0186 55	100	0.000186	0.769
150	0.0073	0.010 110	350	0.0000285	1.266

Table. 2- Thickness dependence of remnant magnetization (M_r), saturation magnetization (M_s), saturation field (H_m), coercivity (H_c), permeability (μ) and the effective anisotropy in Fe/Si(100)

Thichness(nm)	M_r	M_s	H_c	H_m	$\mu=M_s/H_m$	K_{eff}
50	0.00431	0.00425 65		135	0.0000314	0.896
75	0.00668	0.00663 75		150	0.0000442	1.038
100	0.00270	0.00721 40		115	0.0000626	0.906
150	0.01250	0.01312 50		100	0.0001312	1.112

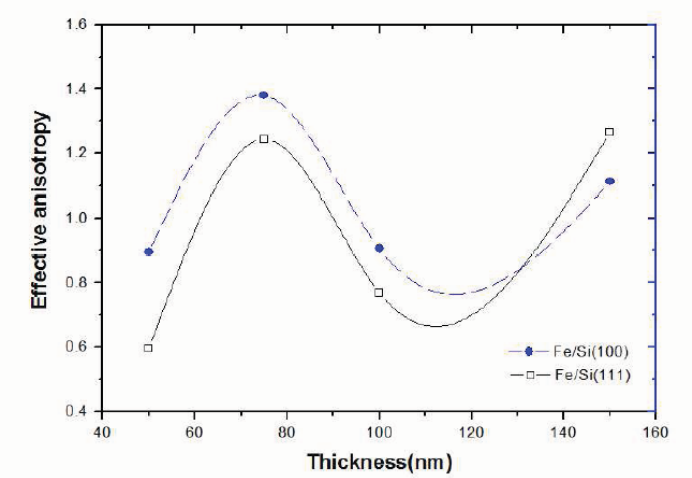

Figure. 5- Thickness dependence of the effective anisotropy in Fe/Si.

Conclusion

The magnetic domain patterns clearly visible in the MFM picture have been taken at the magnetic remanence. MFM results for 100 nm of Fe/Si(111) and Fe/Si(100) substrates are presented. Zoom to part of this images are shown. Domain walls of specimen in 7 *nm* × 7*nm*. Magnetization loops were measured in directions of perpendicular and parallel to the film plane by using AGFM. Hysteresis diagrams show good ferromagnetic characteristics of these samples. The effective anisotropy shows oscillation, for two substrates Si types, when the Fe films thickness increased.

References:

1. Willard, M.A., Laughlin, D.E., McHenry, M.E., Thoma, D., Sickafus, K., Cross, J.O., and Harris, V.G., *J. Appl. Phys.*, **85**, 4421 (1999).
2. Yoshizawa, Y., Oguma, S., Yamauchi, K., *J. Appl. Phys*., **64**, 6044 (1988).
3. Suzuki, K., Makino, A., Inoue, A., Matsumoto, T.*, Matt. Trans. JIM*, **32**, 93 (1991).
4. Alben, R., Becker, J.J., Chi, M.C., *J. Appl. Phys*., **49**, 1653 (1978).
5. Herzer, G., *IEEE Trans. Magn.,* **26**, 1397 (1990).
6. Herzer, G., *Matt. Sci. Eng.*, **133**, 1 (1991).
7. Suzuki, K., Cadogan, J. M., *Phys. Rev.* B, **58**., 2730 (1998).
8. Varga, L.K., Novak, L., Mazaleyrat, F., *J. Mag. Mag. M*att., **210**, L25 (2000).
9. R. A. Hyman, A. Zangwill, and M. D. Stiles, *Phys. Rev.* B, **58**, 9276 (1999).
10. Zhao, D., Liu, F., Huber, D. L., Lagally, M. G., *Phys. Rev.* B, **62**, 11316 (2000).
11. Wulfhekel, W., Knappmann, S., Oepen, H. P., *J. Appl. Phys,* **79**, 988 (1996).
12. Kawakami, R. K., Aparicio, E. J., Qiu, Z. Q., *Phys. Rev. Lett.*,**77**, 2570 (1996).
13. Han, K.-H., Spemann, D., Höhne, R., Setzer, A., Makarova, T.L., Esquinazi, P., and Butz, T., *Carbon*, **41**, 785 (2003).